Comparison of Existing Joint Orientation Parameters and Their Effect on Rock Erodibility in Dam Spillways

Short title: Joint Orientation Parameters and Rock Erosion

M-H.Wisse*[1], A.Saeidi[1], M.Quirion[2]

[1]Applied Sciences, Université du Québec à Chicoutimi, 555 Boul. de l'Université, Chicoutimi, QC, G7H 2B1

[2]Rock Mechanics, Hydro-Québec, 75 Boul. René-Lévesque W, Montréal, QC, H2Z 1A4

*Corresponding author (e-mail: marie-helene.wisse1@uqac.ca)

M-H W.: 0000-0001-7764-5024, AS: 0000-0001-6954-5453, MQ: 0000-0003-2568-6339

Abstract

Rock mass erosion in unlined spillways causes significant structural damage and necessitates expensive repairs. The rock mass is made up of blocks formed by various arrangements of joint sets. The volume and the protrusion of these blocks, as well as the orientation, opening and roughness of the joints, are all features that can affect rock erodibility. Most of these features are incorporated in parameters developed for rock mass characterization. Three joint orientation parameters are compared in this article using a database containing geological and hydraulic information on scoured spillways. According to the detailed methodology, data is first classified according to rock quality using the GSI_{chart} index. Then, for each GSI_{chart} class, data is distributed according to the damage level, stream power and joint orientation parameter chosen. This study shows that no joint orientation parameter is currently able to accurately represent the effect of joint orientation on erosion of excellent- to poor-quality rock mass. Moreover, this study shows that the GSI_{chart} index is not a rock quality index that completely evaluates rock erosion, since some relevant parameters for evaluating rock erodibility are not considered.

Keywords: Joint orientation, erosion, rock mass, hydraulic, unlined spillway

1 Introduction

Hydroelectricity production requires the construction of dams. For safety, emergency spillways are built as part of these dams to carry away excess water. These spillways are excavated into the bedrock, which exposes the rock mass to the erosive power of water flow. In some cases, rock mass erosion in unlined spillways has been shown to cause damage to the dam's structure. The erosion process occurs in all rock mass qualities and is affected by rock mass features and flow characteristics. In the field of rock mechanics, several methods for evaluating rock mass erodibility have been developed, such as those of Kirsten (1982), Van Schalkwyk (1994), Annandale (1995) Kirsten et al. (2000), Bollaert (2004; 2010; 2002) and Pells (2016). These methods fall into two main categories: semi-analytical and semi-empirical (Jalili Kashtiban et al. 2021). The main existing semi-analytical method is the presented by Bollaert (2004; 2010; 2002) – the Comprehensive Scour Model (CSM). Methods of Kirsten (1982), Van Schalkwyk (1994), Annandale (1995), Kirsten et al. (2000) and Pells (2016) are classified as semi-empirical. Semi-empirical methods define a threshold where erosion in a rock mass occurs, i.e., when the stream power becomes greater than a rock's resistance to erosion. Several researchers have sought to find methods to define rock mass resistance to erosion according to its characteristics, such as block size, joint orientation, uniaxial compressive strength, joint opening, joint roughness and joint shear strength. Boumaiza et al. (2021) have developed a methodology to identify the relative impact of each of these features on the hydraulic erodibility of rock. It was found that joint orientation influences rock mass resistance to erosion when subjected to flow power. This article focuses on semi-empirical methods involving a parameter that describes the effect of joint orientation within the flow. Methods involving joint orientation parameters that are compared in this paper are described below.

The Kirsten index (N) is an excavatability rock mass index that is designed to assess the ease of excavating bedrock with a bulldozer (Kirsten 1982). This index has also been used to evaluate the erodibility of the rock mass. However, this application has been criticized. Van Schalkwyk (1994), Annandale (1995), and Kirsten et al. (2000) used the Kirsten index to define a rock erodibility limit. This limit depends on the rock's resistance to erosion, determined using Kirsten's index, and

C_{up}: Uplift pressure coefficient dependent on joint orientation defined through experimental tests.

on the erosive capacity of the flow (Jalili Kashtiban et al. 2021). Kirsten's index is presented in equation (1).

$$N = M_s K_b K_d J_s \qquad (1)$$

Where M_s is the uniaxial compressive strength of the rock, K_b refers to the block size, K_d refers to the shear strength and J_s is the joint orientation parameter. J_s defines a value of the rock's vulnerability to erosion as a function of the joint spacing ratio and the joint orientation within the flow. The Kirsten index was originally designed to define the ease with which a rock mass can be excavated. Since its inception, there has been a lot of criticism of this method. In particular, its application to erodibility situations has been questioned by several authors and some of the parameters used have been shown not to provide a satisfactory estimate of what they represent (Boumaiza 2019; Pells 2016). Boumaiza et al., (2019a) reveals that the estimation of orthogonal joint sets when calculating J_s is inadequate and that a better approximation of the angle between joint sets should be considered. Pells (2016) notes that the M_s and RQD factors of Kirsten's index have a much greater impact on the final value of Kirsten's index. The maximum values of M_s and RQD are 280 and 100, and their minimum values are 0.87 and 5, respectively. In contrast, the maximum and minimum values of the J_s parameter are 1.50 and 0.37. The overall impact of the J_s parameter on Kirsten's index is low.

Pells (2016) proposed two new methods to assess rock mass erodibility: the Rock Mass Erodibility Index (RMEI) and the Erodibility Geological Strength Index (eGSI) (equation 2). It is in the eGSI that he introduces E_{doa} as a new parameter to evaluate the effect of joint orientation on rock mass erodibility. E_{doa} makes it possible to evaluate rock resistance to erosion according to joint orientation and joint spacing ratio. The value of E_{doa} is added to the GSI index developed by Hoek et al. (1995).

$$eGSI = E_{doa} + GSI_{chart} \qquad (2)$$

Pells (2016) used Marinos and Hoek (2000) chart to calculate GSI_{chart}.

Reinius (1986) and Montgomery (1984) studied the effects of the orientation of blocks aligned in a horizontal flow channel. Along with different block dispositions (such as orientation and protrusion) and various flow rates, pressures applied on one of the blocks were measured and the uplift pressure coefficient C_{up} was obtained.

The two main parameters that evaluate the effect of joint orientation are E_{doa} and J_s. However, since C_{up} is also a parameter that vary according to block orientation, it is considered in this study. J_s, E_{doa} and C_{up} do not report the same effect of joint orientation on rock mass erodibility. In order to determine the parameter that best represents the effect of joint orientation on rock mass erodibility, a method was used to assess the applicability and the effectiveness of each joint orientation parameter to classify rock mass according to its vulnerability to erosion. This paper covers the methodology used to define the parameter that best represents the effect of joint orientation, presents a summary of the existing parameters, considers the results obtained and ends with a discussion on the significance and validity of these results.

2 Materials and Methods

The database used in this study was developed by Pells (2016). It includes the description, geomechanical features and several geomechanical parameters of the rock mass in 24 dams located in South Africa and Australia. Flow strength, flow direction and erosion damage levels are also documented. For each dam, the spillway is separated into different sections depending on the damage level. For each section, the following geomechanical parameters of joint sets are described: opening, spacing, persistence, dip, orientation and roughness. The rock is also evaluated with the Kirsten index factors: RQD, J_n, J_r, J_a, J_s and M_s. In total, the database contains information on a total of 114 sections spread across 24 dams. This information was reported in the form of consultant reports, technical documents and observations made by geologists.

The first step of the methodology is to develop the database. E_{doa} and J_s are determined by Pells (2016) for each section. C_{up} is determined according to the most critical joint orientation of each data set. Rock mass quality is assessed by the GSI_{chart} rock resistance index, which is determined by Pells (2016). Stream power and damage levels are also defined by Pells (2016).

The joint orientation parameters were compared together using the eGSI index, which combines a joint orientation parameter to a rock mass quality index. By varying the joint orientation parameter combined with the GSI_{chart}, it is possible compare their effectiveness, given the assumption that eGSI is an effective method to determine erosion.

The methodology used to compare joint orientation parameters was inspired by Boumaiza et al. (2019b). To combine similar data together, as it is a common practice in rock mechanics, each parameter must first be divided into classes: joint orientation parameters, GSI_{chart}, stream power and damage level. For each GSI_{chart} class, a graph of the mean stream power class in relation to the damage level class is produced. Joint orientation parameters are then plotted, according to the joint orientation parameter class. It is then possible to compare the effectiveness of the joint orientation parameter selected according to the damage level recorded. The methodology is summarized in Figure 1.

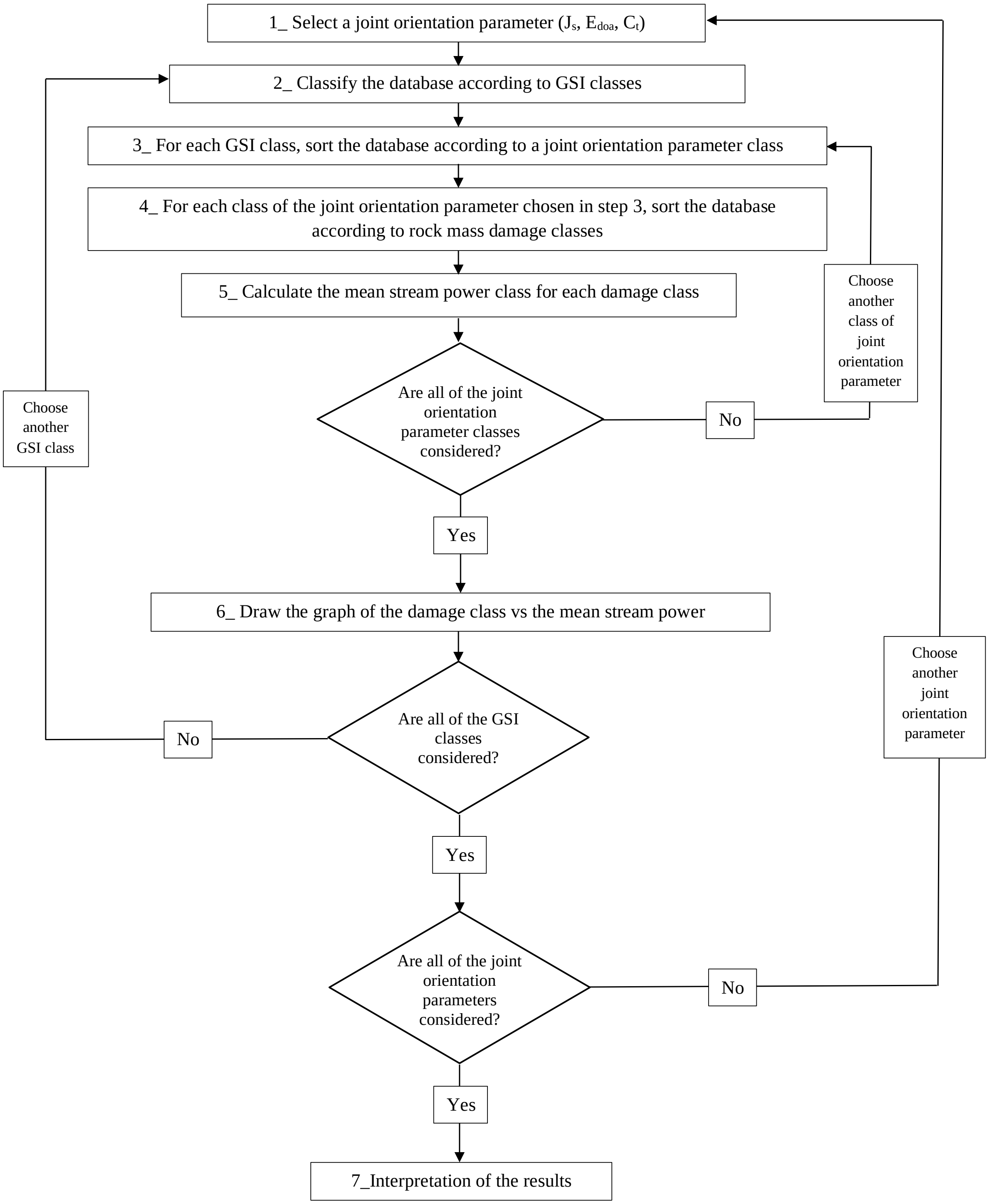
1_ Select a joint orientation parameter (J_s, E_{doa}, C_t)
2_ Classify the database according to GSI classes
3_ For each GSI class, sort the database according to a joint orientation parameter class
4_ For each class of the joint orientation parameter chosen in step 3, sort the database according to rock mass damage classes
5_ Calculate the mean stream power class for each damage class
Are all of the joint orientation parameter classes considered?
No
Choose another class of joint orientation parameter
Yes
6_ Draw the graph of the damage class vs the mean stream power
Are all of the GSI classes considered?
No
Choose another GSI class
Yes
Are all of the joint orientation parameters considered?
No
Choose another joint orientation parameter
Yes
7_Interpretation of the results

2.1 Step 1 – Select a Joint Orientation Parameter

Step 1 consists of selecting one joint orientation parameter from those presented (E_{doa}, J_s or C_{up}). The following steps will be performed according to the selected parameter.

2.2 Step 2 – Classify the Database According to GSI_{chart}

The goal of this step is to combine data with similar rock quality index. GSI_{chart} values are assigned a class from 1 to 4, according to RMR classification (Bieniawski 1989). Classes are assigned according to the separation shown in Figure A.1.1 in Appendix 1.

2.3 Step 3 – Classify the Joint Orientation Parameter Chosen for Each GSI Class

The goal of this step is to group data into different classes according to the value of the joint orientation parameter previously chosen.

2.3.1 J_s Parameter Classification

Classification of J_s was done by Boumaiza et al. (2019b) by statistically distributing Pells (2016) database. Classification of J_s is detailed in Table 1.

2.3.2 E_{doa} Parameter Classification

Classification of E_{doa} was done by Boumaiza et al. (2019b) by statistically distributing Pells (2016) database. Classification of E_{doa} is detailed in Table 2.

2.3.3 C_{up} Parameter Classification

Classification of C_{up} is presented in Table 3. It was done by statistically distributing Pells (2016) database and based on the effect that this parameter has on erosion.

2.4 Step 4 – Classify the Damage Level

The goal of this step is to assemble data with a similar damage level class from data with the same GSI_{chart} class and joint parameter class. The damage level classes were defined using Pells classification (2016). The damage categories depend on the depth of the erosion and its general extent. The classification proposed by Pells (2016) is presented in Table 4.

2.5 Step 5 – Classify the Stream Power

The goal of this step is to group together all data with the same GSI_{chart} class, the same joint orientation parameter class and the same damage class. Mean stream power is calculated using this data. A classification of stream power classes had already been proposed by Boumaiza et al. (2019b). However, this classification did not sufficiently account for the highest stream power, which is greater than 100kW/m^2. This is why a modified classification is proposed, as shown in Table 5.

When all the classes of the chosen joint orientation parameter have been evaluated, continue with step 6. Otherwise, start over with a new joint orientation parameter class in step 3.

2.6 Step 6 – Draw the Damage Class Graph as a Function of the Mean Stream Power Class for the Chosen Joint Orientation Parameter

This step aims to visually compare the effect of each joint orientation parameter on rock mass erodibility. In total, four graphs will be created for each joint orientation parameter, with each graph representing one GSI_{chart} class. The Y-axis represents the damage level class and the X-axis represents the mean stream power class for each class of the joint orientation parameter with the same damage class and GSI_{chart} class.

If all GSI_{chart} classes are considered for the same joint orientation parameter, continue with the next joint orientation parameter and repeat steps 1 to 6. Otherwise, choose a new GSI_{chart} class and repeat steps 2 to 6.

2.7 Step 7 – Interpret the Results

This step involves interpreting the results obtained and determining which joint orientation parameters best represent the effect of joint orientation on rock mass erodibility.

3 Theory

In the following section, the three joint orientation parameters introduced are presented in detail.

3.1 Presentation of the J_s Parameter

The J_s parameter describes the effect of joint orientation on rock mass excavatability according to the direction of excavation. Kirsten (1982) indicates it is easier to excavate a rock which contains joints that dip in the same direction as the excavation rather than the opposite direction. In Kirsten's study (1982), some assumptions are made to evaluate J_s: joint sets are considered orthogonal and only the two closest joint sets are considered. Since Kirsten's index is used to assess rock mass erodiblity rather than excavatability, in this article, J_s is considered to be a joint orientation parameter for rock mass erodibility. The joint spacing ratio (r) is defined by the ratio of S_ψ, the spacing between joints dipping in the opposite direction of ripping, and S_θ, the spacing between joints dipping in the direction of ripping (Figure A.1.2 in Appendix 1). The joint spacing ratio presented in equation 3 is necessary to determine J_s.

$$r = S_\psi / S_\theta \qquad (3)$$

J_s values can be found from Table A.1.1 in Appendix 1. The first step in defining J_s is to define the closest spaced joint set oriented perpendicular to the flow. Then, depending on the dip direction of this joint set (whether it is in the same or opposite direction of the flow), the value of J_s will be found either in the upper section (for 0˚) or in the lower section (for 180˚) of Table A.1.1. With the joint spacing ratio and the dip of this joint set, it is possible to find a value for J_s. When joint orientation has no effect on rock mass erodiblity, J_s is equal to 1. J_s value will decrease below 1 if joint orientation increases a rock's vulnerability to erosion. If joint orientation increases a rock's resistance to erosion, the J_s value will increase to above the value of 1.

3.2 Presentation of the E_{doa} Parameter

Pells (2016) added the E_{doa} parameter to the rock quality index GSI_{chart} (Marinos and Hoek 2000) to consider joint orientation and joint spacing effects on rock erosion, as GSI_{chart} does not take them into account. E_{doa} is based on the results of laboratory tests on a physical model, erosion, geological and hydraulic data of dam sites, and on the theory of block uplift. Pells used the model of the J_s parameter to develop E_{doa}. However, E_{doa} is more precise, considering different parameters such as flow types, channel slopes and various joint spacing ratios (r): 1: 1, 1: 2, 1: 4, 1: 8, 1:20. For a horizontal channel and a bed-parallel flow, E_{doa} presents negative values, with a maximum value of 0 and a minimum value of -18 (Figure 2). Therefore, joint orientation cannot have a positive effect on the resistance to erosion of the rock, as for the J_s parameter.

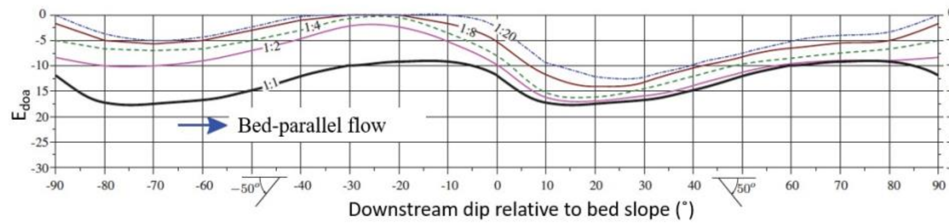

3.3 Presentation of the C_{up} Parameter

The Reinius (1986) and Montgomery (1984) laboratory experiments made it possible to obtain different values of pressure acting on an instrumented block placed in a horizontal flow channel, among an alignment of non-instrumented blocks (Figure 3a). The block was instrumented with 14 piezometers, which were used to measure the hydraulic head at different points (Figure 3b). The block dimensions were 15 x 15 x 30 cm^3. The Reinius (1986) and Montgomery (1984) studies considers various flow rates, water loads above the block and block dips. As shown in Figure 3 (a) and (b) the ß angle is calculated from the vertical, whereas the dip is calculated from the horizontal. In order to compare the parameters, a 90˚ correction was made to transform ß values into dip values.

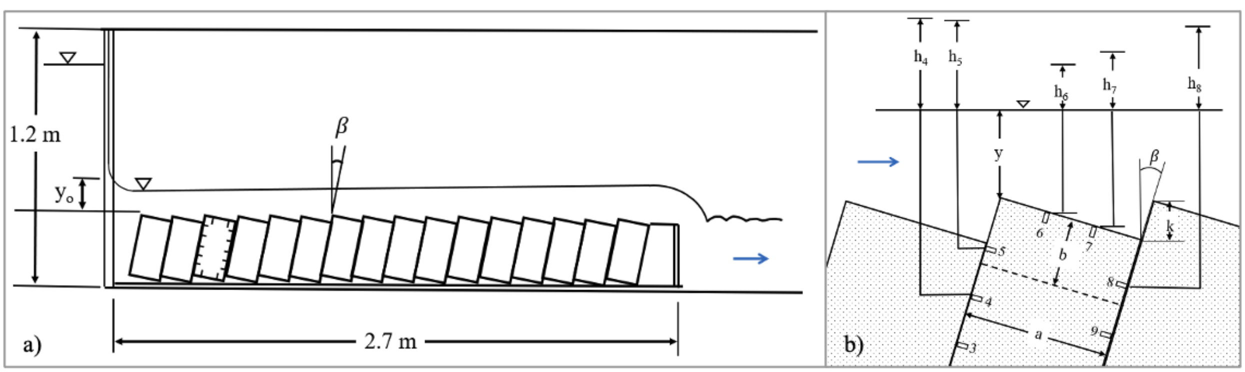

Using piezometer data, a dimensionless pressure coefficient c was obtained (equation 4).

$$c = \frac{h}{U^2/2g} \quad (4)$$

Where h represents the dynamic pressure (m), U represents the velocity of water (m s^{-1}) and g represents the gravitational acceleration (m s^{-2}).

The dynamic pressure h_d is obtained from the water head recorded by the piezometer, from which the static pressure, the height of water from the piezometer, is subtracted (equation 5).

$$h_d = h_t - h_s \quad (5)$$

Where h_t is the piezometer, i.e., the total water pressure, and h_s is the static pressure, the water load above the block. C_{up} was calculated with the mean value of the pressure coefficients at piezometers 5 and 8, when considering a block of thickness *b* (Figure 3 (b)).

4 Results

4.1 Classification of the GSI_{chart} Index

According to the classes shown in Figure 2, GSI_{chart} data distribution is presented in Figure 4 (a). The Y-axis represents the total data for each GSI_{chart} class.

4.2 Classification of the J_s Parameter

Data classification for the J_s parameter was performed according to the classes described in Table 1. Figure 4 (b) shows data distribution for each J_s class. Class 4 of J_s has significantly more data than the other classes. This class corresponds to a J_s equal to one, representing joint orientation having no impact on Kirsten's index, i.e., having no impact on rock resistance. The Y-axis represents total data for each J_s class.

4.3 Classification of the E_{doa} Parameter

Data classification according to the E_{doa} parameter was done according to classes described in Table 2. Figure 4 (c) shows data distribution for each E_{doa} class. The E_{doa} of class 1 has far fewer data than the other classes. This class corresponds to a situation where E_{doa} has the least effect on rock mass resistance to erosion. The Y-axis represents total data for each E_{doa} class.

4.4 Classification of the C_{up} Parameter

In order to assess a C_{up} value for each data set available, each joint set was analyzed according to its orientation in relation to the flow. Only joint sets not parallel to the flow were considered. A joint set must have a difference of orientation of at least 20˚ to be considered valid for this analysis. Then, according to Reinius (1986), the most critical joint set for each data set was chosen. The most critical joint set is the one with the highest C_{up} value. Figure 5 illustrates the distribution of data according to the C_{up} parameter and the orientation ß (˚) of the block. Only the most critical

C_{up} values were retained for each data set. Figure 4 (d) shows data distribution according to these two situations. The Y-axis represents total data for each C_{up} class.

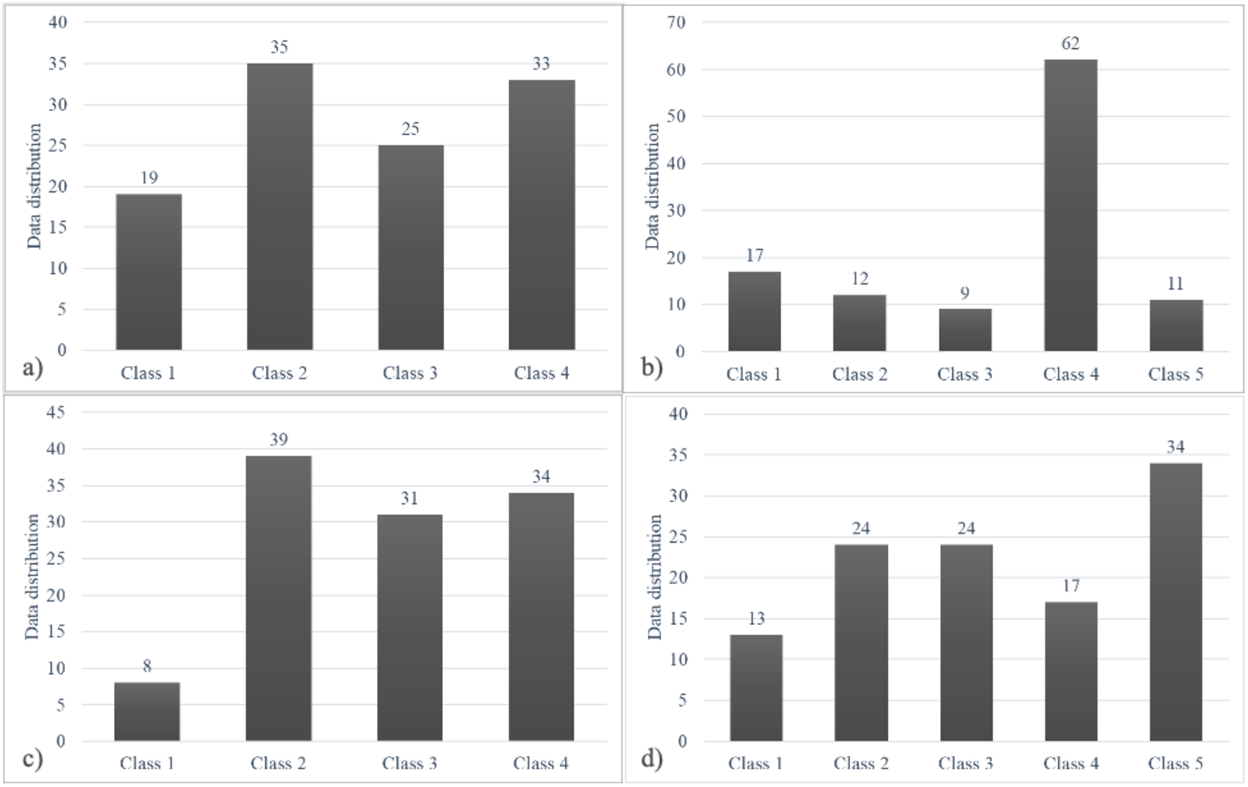

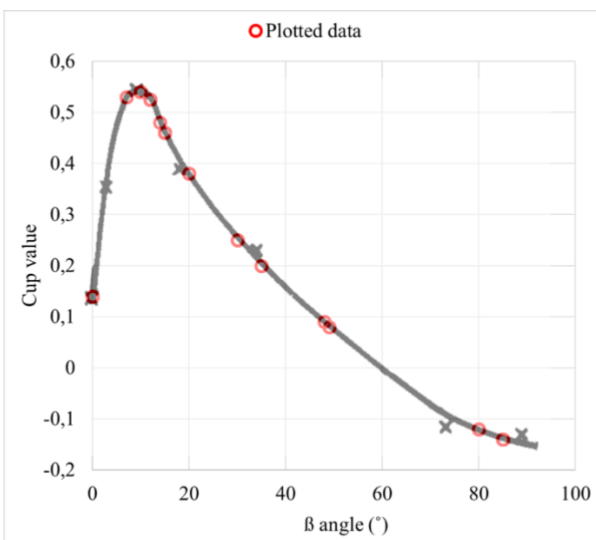

4.5 Effects of J_s on Rock Mass Erosion

The effect of the J_s parameter are shown in Figure 6 (a-d). The Y-axis represents the mean stream power class and X-axis represents the damage level class. The bubble size represent the amount of data for each bubble. J_s of class 1 (Js1) is defined by a joint orientation increasing the rock mass erodibility and J_s of class 5 (Js5) represents a joint orientation increasing rock mass resistance to erosion. If J_s correctly represents the effects of joint orientation on erosion, a high J_s class should produce less damage than a lower class. In addition, the relation between damage classes and the mean stream power class should be linearly increasing.

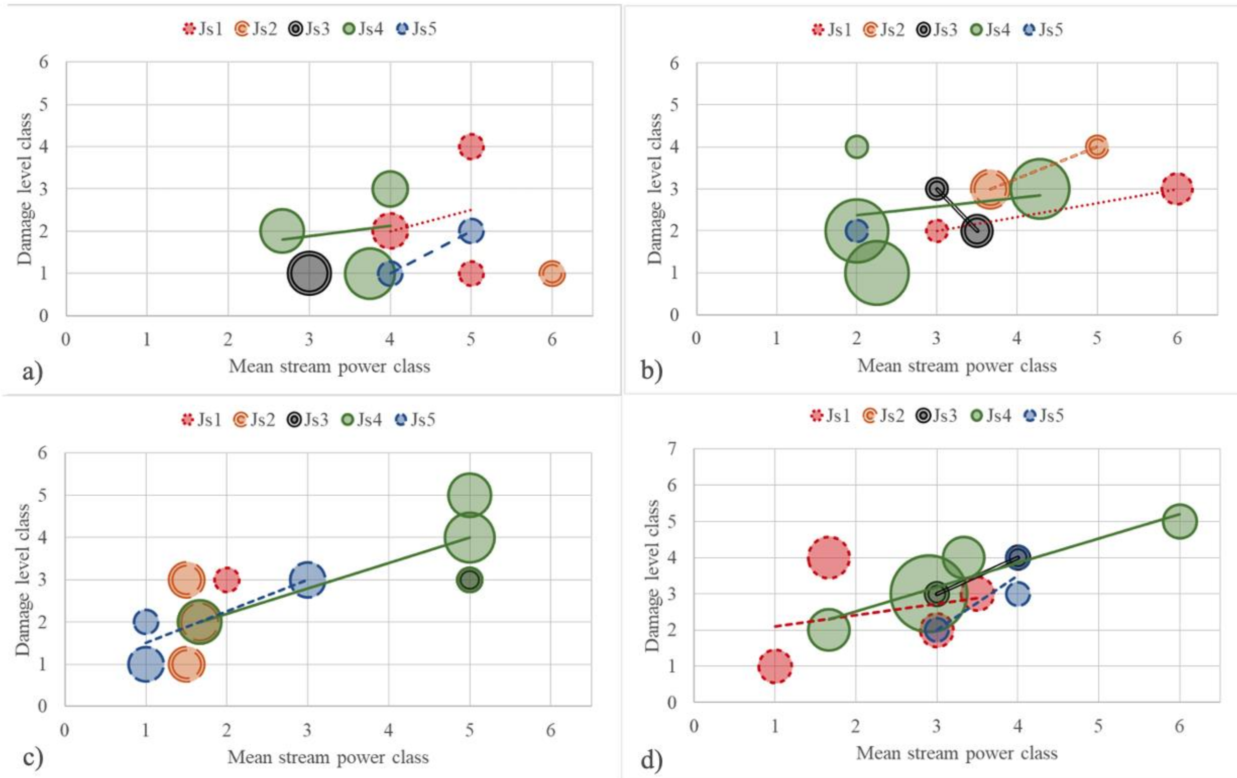

For all GSI_{chart} classes, the majority of the J_s classes do not show the expected relation between them. Indeed, the J_s of class 1 never show more damage than J_s of class 2. We can, however, observe in Figure 6 (b) that the J_s of class 2 show more damage than the J_s of class 4, and for stream power class above 3, more damage than J_s of class 3. Some correlation is observed for J_s of class 4 and 5. J_s of class 4 shows indeed more erosion vulnerability than J_s of class 5, supposed to show erodibility resistance. We can also observe that the majority of the classes show the expected relation between the damage level and mean stream power class, which is observed to be increasing, as expected.

4.6 Effects of the E_{doa} Parameter

The effects of the E_{doa} parameter are shown in Figure 7 (a-d). If the E_{doa} parameter correctly represents the effects of joint orientation on erosion, a higher E_{doa} class should produce more damage than a lower class. In addition, the relation between damage classes and the mean stream power class should be linearly increasing.

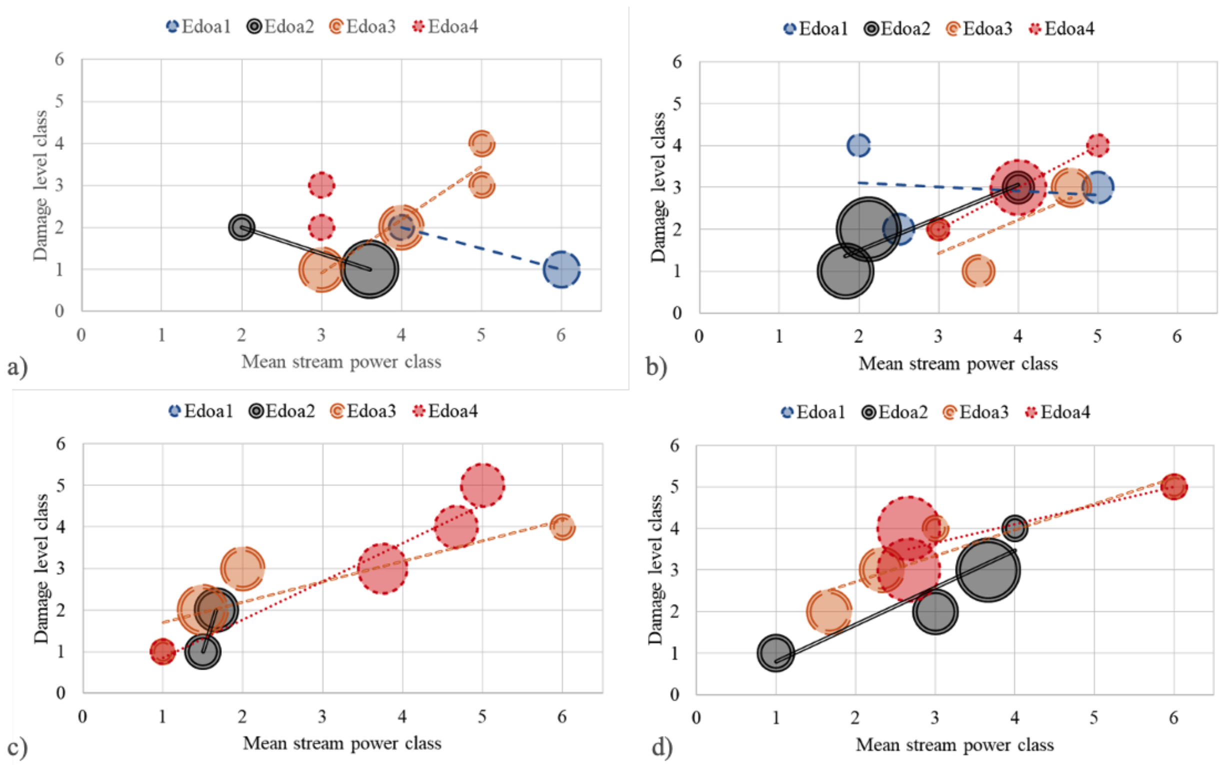

For high rock quality, corresponding to a GSI_{chart} of class 1, the E_{doa} parameter does not show the expected logical relation. For a GSI_{chart} of class 1, in Figure 7 (a), the relation between the damage level and the mean stream power class for E_{doa} of class 1 and class 2 is reversed, when both are expected to be increasing. Aside from this aspect, the relationships between the E_{doa} classes are not respected, with a larger class showing less damage than a smaller class for low to medium stream power. For high stream power, the relation between higher E_{doa} classes is more respected, with higher classes showing more damage than lower classes. For a GSI_{chart} of class 2, in Figure 7 (b), the order of damage level versus E_{doa} classes is respected from a mean stream power of class 4. Lower stream power classes may not generate enough energy for the joint orientation to have a notable impact on rock erosion. The same pattern is observed for GSI_{chart} of class 3, where a good relation between E_{doa} happens when stream power mean class reaches 3. GSI_{chart} class 4 in Figure 7 (d) shows that E_{doa} classes have a logical relationship, both in terms of the order of the E_{doa} classes and of the relationship between damage and stream power.

4.7 Effects of the C_{up} Parameter

The effects of the C_{up} parameter are shown in Figure 8 (a-d). The Y-axis represents the damage level and the X-axis represents the mean stream power class. If the C_{up} parameter correctly represents the effects of joint orientation on erosion, higher classes should show more damage than lower C_{up} classes. In addition, the relation between damage classes and mean stream power should be linearly increasing.

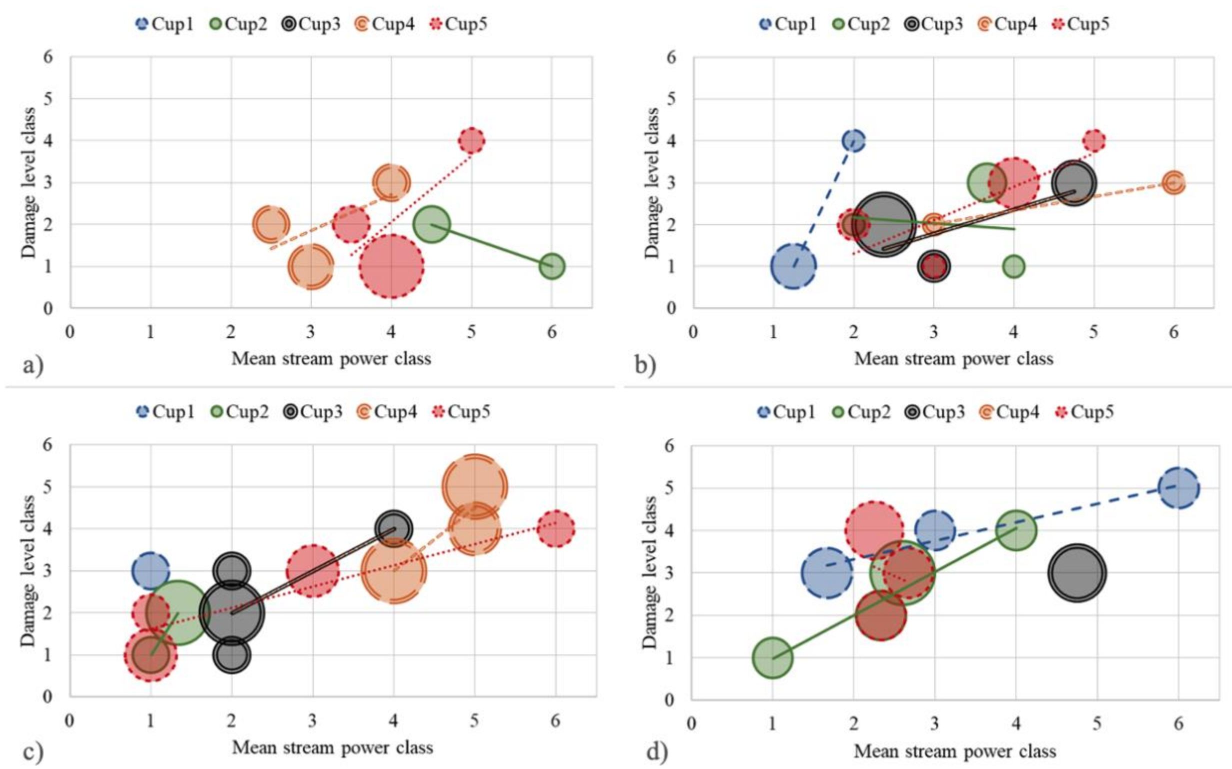

For the GSI_{chart} classes 1 and 2, i.e., for good-quality rock masses, the results show an acceptable classification of the C_{up} parameter. It is generally observed that higher C_{up} classes generate higher damage levels, for high stream power classes. However, for lower-quality rock mass, for GSI classes 3 and 4, correlation between damage and C_{up} classes is no longer observed. It is also noted that the relation between stream power and damage is generally increasing.

4.8 Comparison of Results

In general, the parameter classification results improve as the mean stream power classes increase. For the E_{doa} parameter, its classification also improves when the GSI_{chart} increases. An increase in the GSI_{chart} classes, according to the classification proposed in this article, occurs when the quality of the rock mass decreases. Thus, joint orientation would have a greater impact on erodibility for a lower quality rock subjected to high hydraulic pressures. However, this is counterintuitive since in a very low-quality rock mass i.e., for a GSI_{chart} below 40, corresponding to a GSI_{chart} of class 4, the rock is crushed and joint orientation is not easily distinguished. Joint orientation is best distinguished when rock mass quality is high. Results show correlation between joint orientation and damage level when GSI_{chart} is of class 1 and class 2, for high stream power, only for the C_{up} parameter. No joint orientation parameter presents an accurate relationship between damage level and joint orientation effect for a good quality rock mass. For all GSI_{chart} classes, solely J_s classes 4 and 5 show correlation with damage classes. These classes describe joint orientation that would either have no effect or have a positive effect on rock resistance to erosion.

5 Discussion

There are several methods used to classify the effect of joint orientation in a given rock mass on its erodibility. These methods offer different classifications, hence the need to evaluate these methods and compare their accuracy.

The errors in the classification of the J_s parameter developed by Kirsten (1982) can be explained by four factors, namely the assumption that joints are orthogonal to each other, the fact that J_s parameter has been developed to characterize the excavatability of the rock rather than erodibility, the fact that this parameter was developed only theoretically, and the poor amount of data for all J_s classes except for J_s of class 4 (Figure 6). Boumaiza et al (2019a) show that the approximation of orthogonal joints leads to significant errors when calculating Kirsten's index when the joint sets considered are in fact non-orthogonal. J_s is obtained with the direction of the closer spaced joint set and the apparent dip of the closer spaced joint set with relation to the direction of the flow. However, the apparent dip is calculated considering the two joint sets as being orthogonal. If they are in fact non-orthogonal, this apparent dip will change along with the J_s value. In addition, Kirsten's index, considering the J_s parameter, was developed to characterize the excavatability of a rock mass. The force considered when excavating a rock mass is that of a bulldozer, where the force applied by the excavator acts only at a specific point and is directed at a specific angle. The study of erodibility by hydraulic power involves a hydraulic force acting on all the faces of the blocks of the rock mass, particularly with an uplift force that acts under the block. Since this parameter was developed wholly theoretically, some inconsistencies may have appeared, like the fact that joint orientation can have a positive effect on rock resistance to erosion. Since this methodology was applied on a limited data set, data was unequally distributed through J_s classes, which resulted in too few data for four out of five of J_s classes.

The E_{doa} parameter was developed by Pells (2016). It is based on the J_s parameter, the results of tests on a scale model, real erosion situations that have taken place in dams and on the kinematics of block uplift. Pells (2016) physical model has flaws regarding the analysis of joint orientation effects. Indeed, only one block is modelled, not allowing to measure the effect that joint orientation could have on a series of blocks and joints. Multiple blocks and joints surrounding an instrumented block could have an incidence on the uplift pressure measured on that block. Also, only a few orientations were tested, that is 0°, 22° and 45° horizontally and 0°, 11° and 22° vertically. Horizontal and vertical orientations correspond to direction and to dip direction, respectively. The E_{doa} parameter also considers orthogonal joints, which presents the same problem as for the J_s parameter. Pells (2016) built his database with erosion and dam data coming from different sources. Since Pells (2016) did not collect all data himself, some errors or different interpretations coming from different sources could have been included, especially regarding more qualitative parameters, such as GSI_{chart}. An analysis of the results demonstrates that the E_{doa} parameter offers the best classification of the joint orientation effect on rock mass erodibility. However, the database used to build the E_{doa} parameter was used for this study, which could introduce bias into the results of E_{doa}.

The C_{up} parameter of Reinius (1986) is exclusively based on the pressure results obtained from a scale model. The advantage of the C_{up} parameter is that it is the only parameter based exclusively on laboratory tests. It is, therefore, possible to precisely understand its origin. The physical model used consisted of an alignment of blocks, one of which was instrumented with piezometers. The uplift pressure parameter is not calculated directly from the pressures measured under the block, but is calculated as the mean value of the pressure coefficients of piezometers 5 and 8. Moreover, pressure variation was not measured as a variable dependent of time, more as a fixed value for each model setup. The C_{up} parameter yields opposite results to the E_{doa} parameter, with a better correlation for high GSI classes. In Reinius (1986) experiments to development the C_{up} parameter, the rock mass was modelled with concrete blocks. These blocks thus represent a rock mass of high quality, which corresponds with GSI classes 1 and 2. Therefore, the C_{up} parameter may only be applicable to good GSI classes. Unlike E_{doa} and J_s, C_{up} does not consider joint spacing. The joint spacing considered for the C_{up} parameter is the one used in Reinius (1986) experiments, which is has a fixed value for all tests. According to E_{doa} and J_s, joint spacing does not radically change the impact of joint orientation, but it does change the value slightly. Additionally, joint orientation testing by Reinius (1986) was limited. The block was always placed vertically in the model, with varying dips from the vertical of 0˚, 9˚, 17.5˚, and 33.5˚ in the opposite direction of the flow and varying dips from the vertical of 2.9˚ and 18˚ in the same direction of the flow. These tests allowed Reinius (1986) to extrapolate his results to all cases. However, the C_{up} parameter would need to be further developed in order to be applied to all cases of joint orientation.

This study reveals some probable inconsistencies with the GSI_{chart} determination in relation to joint orientation. Considering the joint orientation parameters analyzed, results show that joint orientation has much less of an effect on good-quality rock mass than on lower-quality rock mass. However, joint orientation is much more distinguishable on a good quality rock mass. GSI_{chart} is determined using block structure and joint condition. When considering GSI_{chart}, the same GSI_{chart} value is determined for a "very blocky" rock mass with a good joint condition (rough and not altered) as for a "massive" rock mass with a medium joint condition (smooth and altered), which could explain the issue regarding the effect of joint orientation. To effectively compare the effect of joint orientation, rock mass should be classified according to the same class of structure and the same class of joint condition. Moreover, in our analysis with GSI_{chart}, joint orientation and stream power does not consider all parameters as having an effect on rock mass erosion, such as NPES and joint opening. Boumaiza et al (2021) revealed a classification of the most relevant parameters to study rock mass hydraulic erodibility. From the most to the least important, his study obtained the following classification: joint condition (K_d), nature of the potentially erodible surface (NPES), block volume (V_b), joint opening (J_o), joint orientation (E_{doa}) and rock mass deformation module (E_{rm}). Our study does not consider NPES, which includes the block's protrusion, nor does it consider joint opening or rock deformation module. It would be interesting to include NPES and J_o in an index of rock quality, as they have more importance for rock mass hydraulic erosion than joint orientation. Furthermore, joint condition and block volume have the same weight when determining GSI_{chart}, when, according to Boumaiza et al (2021), joint condition is the most important parameter for rock mass hydraulic erodibility with block volume following in third position. Therefore, when studying rock mass hydraulic erodibility, a rock quality index that takes this classification into account should be considered.

6 Conclusion

Hydroelectric facilities require the excavation of an emergency spillway in the bedrock, which exposes the rock mass to hydraulic erosion. Joint orientation is known as a relevant geomechanical parameter to evaluate rock mass erodibility. The method used in this article to evaluate the parameters describing the effects of joint orientation on rock mass erodibility is based on the one used by Boumaiza et al (2019b). The results show that the E_{doa} parameter is the joint orientation parameter with a classification that is closest to expectations, based on the GSI_{chart} index of rock quality, mean stream power and damage level. The E_{doa} parameter shows good correlation when the rock is of medium to low quality. Good results for the E_{doa} parameter may be influenced due to the database used to determine E_{doa} being the same used to analyze its accuracy in our study. This leaves room for potential bias. Regarding the J_s parameter, the classification obtained is not representative of the damage level. However, little data is available for J_s classes 1, 2, 3 and 5, since the majority of data falls under J_s class 4. Regarding the C_{up} parameter, for high stream power, results generally show good correlation for GSI_{chart} classes 1 and 2. Unlike the E_{doa} and J_s parameters, C_{up} does not consider spacing ratio of joint sets, which could help increase the accuracy of the results for this parameter.

Good-quality rock masses can have a variety of structures, from massive to very blocky, with a joint condition ranging from rough and non-altered to smooth and altered. In this study, some parameters that have a significant impact on rock mass erodibility were disregarded, such as NPES, J_o and E_{rm}. Development of a rock quality index that includes these parameters and considers their relative importance would be useful in order to correctly analyze joint orientation parameters and rock mass erodibility.

7 Acknowledgments

The authors would like to thank the research group R^2Eau for their helpful comments and suggestions.

8 Authors contribution

Marie-Hélène Wisse: Conceptualization, Validation, Visualization, Formal analysis, Investigation, Methodology, Writing – Original Draft, Writing – Review and Editing
Ali Saeidi: Conceptualization**,** Methodology, Resources, Writing – Review and Editing, Supervision, Project administration, Funding acquisition, Validation
Marco Quirion: Writing – Review and Editing, Supervision, Funding acquisition

9 Funding

This work was supported by the Natural Sciences and Engineering Research Council of Canada (NSERC) (#RDCPJ 537350 – 18), Mitacs Inc. (# IT22640), Hydro-Québec and Uniper.

10 Data Availability Statement

All data generated or analysed during this study are included in this published article: (Pells 2016).

11 References

Annandale, G.W. 1995. Erodibility. Journal of Hydraulic Research, **33**(4): 471-494. doi:https://doi.org/10.1080/00221689509498656.

Bieniawski, Z.T. 1989. Engineering rock mass classifications: a complete manual for engineers and geologists in mining, civil, and petroleum engineering. John Wiley & Sons.

Bollaert, E. 2004. A comprehensive model to evaluate scour formation in plunge pools. International Journal on Hydropower and Dams, **11**(1): 94-102. Available from https://www.aquavision-eng.ch/index_htm_files/Bollaert_2004.pdf [accessed 01-12-2020].

Bollaert, E. The comprehensive scour model: Theory and feedback from practice. *In* 5th International Conference on Scour and Erosion, San Francisco. 2010. pp. 465-480.

Bollaert, E., and Schleiss, A. 2002. Transient water pressures in joints and formation of rock scour due to high-velocity jet impact. Thesis, EPFL-LCH.

Bollaert, E., Annandale, G., and Schleiss, A. 2002. Scour of rock due to high-velocity jet impact: a physically based scour model compared to Annandale's erodibility index method.

Boumaiza, L. 2019. Rock mass parameters governing the hydraulic erodibility of rock in unlined spillways. Ph.D Thesis, UQAC.

Boumaiza, L., Saeidi, A., and Quirion, M. 2019a. Determining relative block structure rating for rock erodibility evaluation in the case of non-orthogonal joint sets. Journal of Rock Mechanics and Geotechnical Engineering, **11**(1): 72-87. doi:10.1016/j.jrmge.2018.06.010.

Boumaiza, L., Saeidi, A., and Quirion, M. 2019b. A method to determine relevant geomechanical parameters for evaluating the hydraulic erodibility of rock. Journal of Rock Mechanics and Geotechnical Engineering, **11**(5): 1004-1018. doi:https://dx.doi.org/doi:10.1016/j.jrmge.2019.04.002.

Boumaiza, L., Saeidi, A., and Quirion, M. 2021. A method to determine the relative importance of geological parameters that control the hydraulic erodibility of rock. Quarterly Journal of Engineering Geology and Hydrogeology, **54**(4): 2020-2154. doi:https://doi.org/10.1144/qjegh2020-154.

Hoek, E., Kaiser, P.K., and Bawden, W.F. 1995. Support of underground excavations in hard rock. 1st ed. Balkema, Rotherdam, Netherlands.

Jalili Kashtiban, Y., Saeidi, A., Farinas, M.-I., and Quirion, M. 2021. A Review on Existing Methods to Assess Hydraulic Erodibility Downstream of Dam Spillways. Water, **13**(22): 3205. doi:https://doi.org/10.3390/w13223205.

Kirsten, H. 1982. A classification system for excavation in natural materials. Civil Engineer in South Africa, **24**(7): 293-308.

Kirsten, H.A., Moore, J.S., Kirsten, L.H., and Temple, D.M. 2000. Erodibility criterion for auxiliary spillways of dams. International Journal of Sediment Research, **15**(1): 93-107. Available from https://pubag.nal.usda.gov/catalog/22534 [accessed 02-11-2020].

Marinos, P., and Hoek, E. 2000. GSI: A Geologically Friendly Tool For Rock Mass Strength Estimation. *In* ISRM International Symposium, Melbourne, Australia.

Montgomery, R.A. 1984. Investigations into rock erosion by high velocity water flows. Dissertation, University of Washington, Stockholm.

Pells, S. 2016. Erosion of Rocks in Spillways. Thesis, Civil and Environmental Engineering, University of New South Wales.

Reinius, E. 1986. Rock erosion. International Water Power and Dam Construction, **38**(6): 43-48.

Van Schalkwyk, A., Jordaan, J., and Dooge, N. 1994. Erosion of rock in unlined spillways. *In* International Commission on Large Dams. Paris 1994. pp. 555-571.

Table 1. *J_s proposed classification (Boumaiza et al. 2019b)*

Class	**J_s**	**Description**
1	0.4-0.6	Highly vulnerable to erosion
2	0.6-0.8	Very vulnerable to erosion
3	0.8-<1	Moderately vulnerable to erosion
4	1	Less vulnerable to erosion
5	>1	Minimally vulnerable to erosion

Table 2. *E_{doa} proposed classification (Boumaiza et al. 2019b)*

Class	**E_{doa}**	**Description**
1	0 to -5	Minimally vulnerable to erosion
2	-5 to -10	Less vulnerable to erosion
3	-10 to -15	Moderately vulnerable to erosion
4	-15 to -25	Highly vulnerable to erosion

Table 3. *C_{up} proposed classification*

Class	**C_{up}**	**Description**
1	<0	Minimally vulnerable to erosion
2	0-0.1	Less vulnerable to erosion
3	0.1-0.4	Moderately vulnerable to erosion
4	0.4-0.5	Very vulnerable to erosion
5	>0.5	Highly vulnerable to erosion

Table 4. *Proposed classification of damage levels (Pells 2016)*

Class	**Scour depth (m)**	**General extent m^3 $100m^{-2}$**	**Damage description**
1	<0.3	<10	Negligible
2	0.3 - 1	10 - 30	Minor
3	1 - 2	30 - 100	Moderate
4	2 – 7	100 - 350	Large
5	>7	>350	Extensive

Table 5. *Proposed stream power classification. Modified from Boumaiza et al (2019b)*

Class	**Stream Power ($\prod_{uD}$, kW m^{-2})**	**Description**
1	< 2.5	Very Low
2	2.5 - 10	Low
3	10 - 25	Moderate

4	25 - 50	High
5	50 - 100	Very High
6	> 100	Extreme

Table in the Appendix

Table A.1.1. *Relative ground structure number (Js) proposed values rebuilt from Kirsten (1982)*

Dip direction of closer spaced joint set (˚)	**Dip angle of closer spaced joint set (˚)**	**Ratio of joint spacing (r)**			
		1:1	1:2	1:4	1:8
180/0	90	1	1	1	1
0	85	0.72	0.67	0.62	0.56
0	80	0.63	0.57	0.50	0.45
0	70	0.52	0.45	0.41	0.38
0	60	0.49	0.44	0.41	0.37
0	50	0.49	0.46	0.43	0.40
0	40	0.53	0.49	0.46	0.44
0	30	0.63	0.59	0.55	0.53
0	20	0.84	0.77	0.71	0.68
0	10	1.22	1.10	0.99	0.93
0	5	1.33	1.20	1.09	1.03
0/180	0	1	1	1	1
180	5	0.72	0.81	0.86	0.90
180	10	0.63	0.70	0.76	0.81
180	20	0.52	0.57	0.63	0.67
180	30	0.49	0.53	0.57	0.59
180	40	0.49	0.52	0.54	0.56
180	50	0.53	0.56	0.58	0.60
180	60	0.63	0.67	0.71	0.73
180	70	0.84	0.91	0.97	1.01
180	80	1.22	1.32	1.40	1.46
180	85	1.33	1.39	1.45	1.50
180	90	1	1	1	1

Fig. 1: Methodology for comparing joint orientation parameters

Fig. 2: E_{doa} values for a horizontal channel and a bed-parallel flow (Pells 2016)

Fig. 3: (a) Experimental setup. Reworked from Reinius (1986) (b) Simulated fracture between piezometers 5 and 8. Dynamic pressures are also shown. Reworked from Reinius (1986)

Fig. 4: (a) Distribution of data by GSI_{chart} class (b)Distribution of J_s classes of Pells (2016) case studies data (c) Distribution of E_{doa} classes of Pells (2016) case studies data (d) Distribution of data according to Reinius' study. Modified from Reinius (1986)

Fig. 5: Distribution of Pells' (2016) data by C_{up} classification

Fig. 6: Results of the effects of the J_s parameter on the rock's vulnerability to erosion. Lines represent the linear approximation of data distribution (a) GSI_{chart} class 1 (b) GSI_{chart} class 2 (c) GSI_{chart} class 3 (d) GSI_{chart} class 4

Fig. 7: Results of the effects of the E_{doa} parameter on the rock's vulnerability to erosion. Lines represent the linear approximation of data distribution (a) GSI_{chart} class 1 (b) GSI_{chart} class 2 (c) GSI_{chart} class 3 (d) GSI_{chart} class 4

Fig. 8 Results of the effects of the C_{up} parameter on the rock's vulnerability to erosion. Lines represent the linear approximation of data distribution (a) GSI_{chart} class 1 (b) GSI_{chart} class 2 (c) GSI_{chart} class 3 (d) GSI_{chart} class 4

Figures in the Appendix

Fig. A.1.1: GSI determination chart and class separation modified from Marinos and Hoek (2000)

Fig. A.1.2: Sketch of fractured rock mass (Kirsten 1982)

Appendix 1

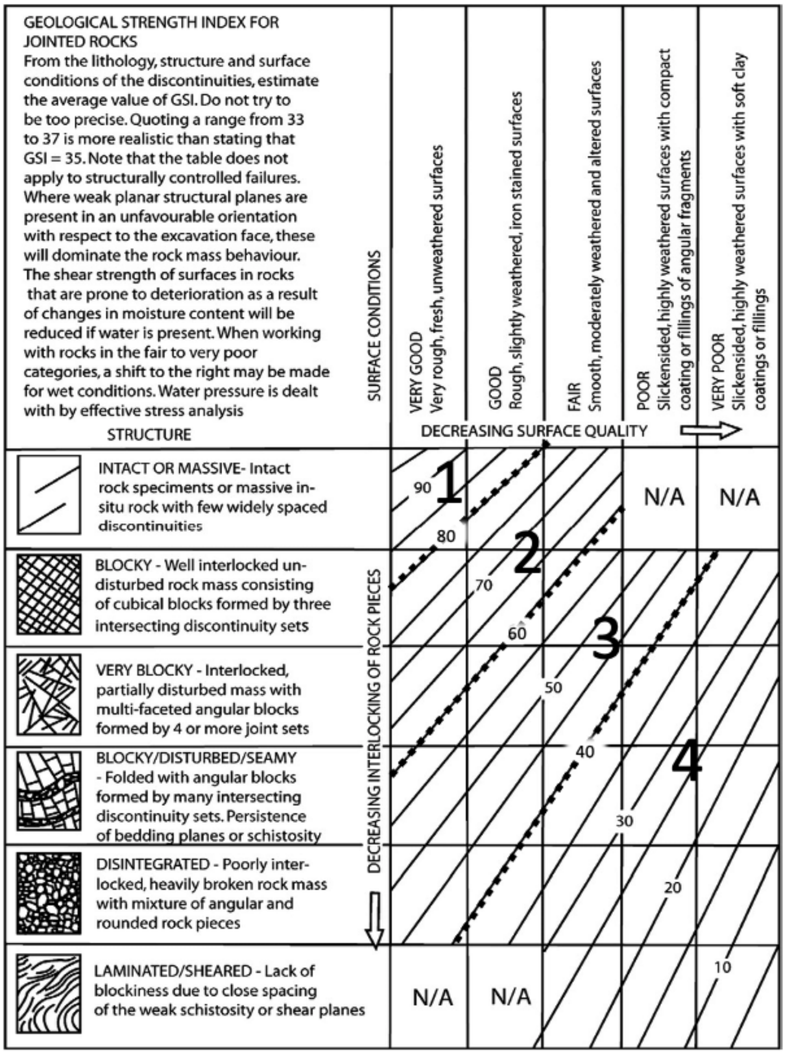
GEOLOGICAL STRENGTH INDEX FOR JOINTED ROCKS
From the lithology, structure and surface conditions of the discontinuities, estimate the average value of GSI. Do not try to be too precise. Quoting a range from 33 to 37 is more realistic than stating that GSI = 35. Note that the table does not apply to structurally controlled failures. Where weak planar structural planes are present in an unfavourable orientation with respect to the excavation face, these will dominate the rock mass behaviour. The shear strength of surfaces in rocks that are prone to deterioration as a result of changes in moisture content will be reduced if water is present. When working with rocks in the fair to very poor categories, a shift to the right may be made for wet conditions. Water pressure is dealt with by effective stress analysis
STRUCTURE
SURFACE CONDITIONS
VERY GOOD Very rough, fresh, unweathered surfaces
GOOD Rough, slightly weathered, iron stained surfaces
FAIR Smooth, moderately weathered and altered surfaces
POOR Slickensided, highly weathered surfaces with compact coating or fillings of angular fragments
VERY POOR Slickensided, highly weathered surfaces with soft clay coatings or fillings
DECREASING SURFACE QUALITY
INTACT OR MASSIVE- Intact rock speciments or massive in-situ rock with few widely spaced discontinuities
BLOCKY - Well interlocked un-disturbed rock mass consisting of cubical blocks formed by three intersecting discontinuity sets
VERY BLOCKY - Interlocked, partially disturbed mass with multi-faceted angular blocks formed by 4 or more joint sets
BLOCKY/DISTURBED/SEAMY - Folded with angular blocks formed by many intersecting discontinuity sets. Persistence of bedding planes or schistosity
DISINTEGRATED - Poorly inter-locked, heavily broken rock mass with mixture of angular and rounded rock pieces
LAMINATED/SHEARED - Lack of blockiness due to close spacing of the weak schistosity or shear planes
DECREASING INTERLOCKING OF ROCK PIECES
N/A
N/A
N/A
N/A
90
80
70
60
50
40
30
20
10
1
2
3
4

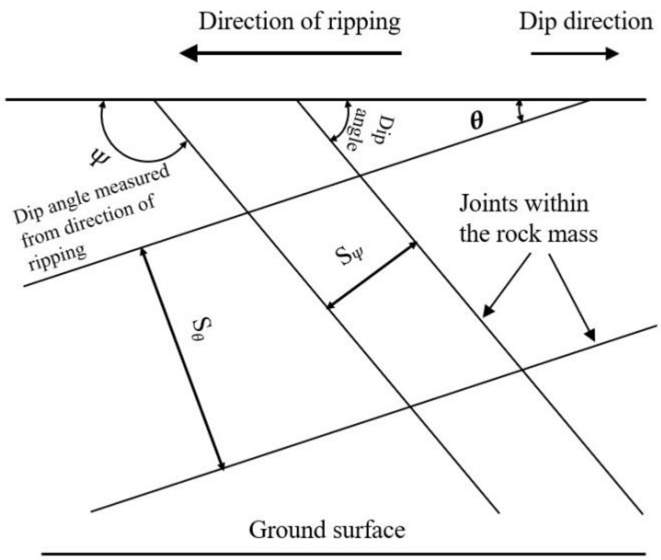

Dip direction of closer spaced joint set (˚)	**Dip angle of closer spaced joint set (˚)**	**Ratio of joint spacing (r)**			
		1:1	1:2	1:4	1:8
180/0	90	1	1	1	1
0	85	0.72	0.67	0.62	0.56
0	80	0.63	0.57	0.50	0.45
0	70	0.52	0.45	0.41	0.38
0	60	0.49	0.44	0.41	0.37
0	50	0.49	0.46	0.43	0.40
0	40	0.53	0.49	0.46	0.44
0	30	0.63	0.59	0.55	0.53
0	20	0.84	0.77	0.71	0.68
0	10	1.22	1.10	0.99	0.93
0	5	1.33	1.20	1.09	1.03
0/180	0	1	1	1	1
180	5	0.72	0.81	0.86	0.90
180	10	0.63	0.70	0.76	0.81
180	20	0.52	0.57	0.63	0.67
180	30	0.49	0.53	0.57	0.59
180	40	0.49	0.52	0.54	0.56
180	50	0.53	0.56	0.58	0.60
180	60	0.63	0.67	0.71	0.73
180	70	0.84	0.91	0.97	1.01
180	80	1.22	1.32	1.40	1.46
180	85	1.33	1.39	1.45	1.50
180	90	1	1	1	1